Acta Crystallographica Section D
**Biological Crystallography**
ISSN 0907-4449

# Structure of the *Rhizomucor miehei* aspartic proteinase complexed with the inhibitor pepstatin A at 2.7 Å resolution

**Jian Yang and J. Wilson Quail***

Department of Chemistry, University of Saskatchewan, 110 Science Place, Saskatoon, Saskatchewan S7N 5C9, Canada

Correspondence e-mail: quail@sask.usask.ca

Received 24 July 1998
Accepted 26 October 1998

**PDB Reference:** RMP–pepstatin A complex, 2rmp.

Crystals of *Rhizomucor miehei* aspartic proteinase (RMP) complexed with pepstatin A grew in the orthorhombic space group $P2_12_12_1$ and were isomorphous to native RMP crystals. The unit-cell dimensions are $a = 41.52$, $b = 50.82$, $c = 172.71$ Å. There is one RMP–pepstatin A complex per asymmetric unit. The structure of the RMP–pepstatin A complex has been refined to a crystallographic $R$ value of 19.3% and an $R_{\rm free}$ value of 28.0% at 2.7 Å resolution. A pepstatin A molecule fits into the large substrate-binding cleft between the two domains of RMP in an extended conformation up to the alanine residue at the P2′ position. The dipeptide analogue statine residue at the P3′–P4′ position forms an inverse $\gamma$-turn (P3′–P1′) with the statine residue at the P1–P1′ position and its leucyl side chain binds back into the S1′ subsite. The inhibitor interacts with the residues of the substrate-binding pocket by both hydrogen bonds and hydrophobic interactions. The hydroxyl group of the statine residue at the P1–P1′ position forms hydrogen bonds with both catalytic aspartate residues (Asp38 and Asp237). This conformation mimics the expected transition state of the enzyme–substrate interaction. The binding of the inhibitor to the enzyme does not produce large distortions of the active site. No domain movement was observed compared with the native enzyme structure. However, the surface-flap region (residues 82–88) undergoes a conformational change, moving toward the inhibitor and becoming rigid owing to the formation of hydrogen bonds with the inhibitor. *B*-factor calculations of the two domains suggest that the C-terminal domain becomes more rigid in the complex than in the native structure.

## 1. Introduction

Aspartic proteinases (E.C. 3.4.23) are a group of proteolytic enzymes, so called because of the presence of two catalytically essential aspartate residues at the active site. Most of them are active at acidic pH and are inhibited by pepstatin, a pentapeptide produced by *Streptomyces* (Umezawa *et al.*, 1970). The chemical structure of pepstatin A is shown in Fig. 1. Aspartic proteinases can be broadly divided into two groups: pepsin-like aspartic proteinases and retroviral aspartic proteinases. The pepsin-like aspartic proteinases are monomers and contain 320–361 amino-acid residues, while the retroviral aspartic proteinases contain 99–150 residues and form a dimer to carry out the catalytic reactions.

During the past 15 years, aspartic proteinase–inhibitor complexes have been extensively studied in order to determine the catalytic mechanism of this group of enzymes (James & Sielecki, 1985; Suguna *et al.*, 1987; Foundling, Cooper, Watson, Cleasby *et al.*, 1987; Foundling, Cooper, Watson, Pearl

*et al.*, 1987; Cooper *et al.*, 1989; Abad-Zapatero *et al.*, 1991; Hoover *et al.*, 1991; Pitts *et al.*, 1995). These results show that the inhibitors fit into the substrate-binding cleft in extended conformations. The residue at P1 (or P1–P1′) of the inhibitor interacts with the two catalytic aspartates by hydrogen bonding; this type of interaction resembles the tetrahedral intermediate in proteolytic cleavage of the peptide bond (Veerapandian *et al.*, 1992).

Recently, the crystal structures of *Rhizomucor miehei* aspartic proteinase (RMP; PDB code 2ASI; Yang *et al.*, 1997; Quail *et al.*, 1998) and *Mucor pusillus* aspartic proteinase (MPP; PDB code 1MPP; Newman *et al.*, 1993) were determined. Three-dimensional structural alignment studies (Yang *et al.*, 1997) show that these two enzymes are closely related, but differ significantly from the known structures of aspartic proteinases from both the pepsin-like and retroviral groups. The sequence alignment of RMP and MPP with other aspartic proteinases (Baudys *et al.*, 1988) also show that RMP and MPP have a sequence identity of 83% with each other and only 22–24% sequence identity with other aspartic proteinases (Newman *et al.*, 1993). These observations indicate that RMP and MPP diverged from other aspartic proteinases at an early stage of evolution and form a subfamily of the aspartic proteinases (Newman *et al.*, 1993; Yang *et al.*, 1997). No structures of RMP or MPP complexes with inhibitors have been published previously. The present study will be the first enzyme–inhibitor complex structure of this subfamily of aspartic proteinases. This research will improve our knowledge of the aspartic proteinases in this subfamily.

## 2. Experimental

### 2.1. Crystallization and data

The purified RMP was provided by Dr Palle Schneider, Novo Nordisk, Denmark (Jia *et al.*, 1995). Pepstatin A was purchased from Calbiochem-Behring Corp., USA. Small thin needle-like seed crystals (<0.01 mm thick) of the native enzyme were grown by the hanging-drop vapour-diffusion method with 25 mg ml$^{-1}$ RMP solution (20 m*M* citrate buffer pH 3.6, 8% PEG 8000) suspended over 26% PEG 8000 reservoir solution (20 m*M* citrate buffer pH 3.6). Aliquots of 10 µl precipitation solution (20 m*M* citrate buffer pH 3.6, 26% PEG 8000) were mixed with 20 µl aliquots containing protein (25 mg ml$^{-1}$ RMP, 0.45 mg ml$^{-1}$ pepstatin A, 2 m*M* citrate buffer pH 3.6). The seed crystals were soaked in this mixed RMP/pepstatin A drop to allow pepstatin A to diffuse into the RMP crystals. The seed crystals were washed to activate the surface and then returned to mixed protein drops to equilibrate over the precipitant solution. After about one month, the crystals with pepstatin A molecules soaked into the active sites of RMP molecules had grown a little larger. These larger crystals were washed and used as seeds for another cycle of reseeding. Repeated combinations of washing and reseeding (Thaller *et al.*, 1981) were carried out by the sandwich-drop method to grow larger crystals. The crystals grew rapidly in two dimensions, but their thickness increased very slowly. Large crystals were cut to smaller dimensions in the washing step to improve the ratio between the crystal dimensions. The crystals used for data collection (0.40 × 0.25 × 0.05 mm) were obtained after five cycles of this combination of washing and reseeding. The crystals of the RMP–pepstatin A complex grew in the orthorhombic space group $P2_12_12_1$. The unit-cell dimensions are $a$ = 41.52, $b$ = 50.82, $c$ = 172.71 Å. There is one RMP–pepstatin A complex per asymmetric unit. The unit cell of the complex is slightly smaller than that of the isomorphous native RMP enzyme ($a$ = 41.82, $b$ = 51.21, $c$ = 174.24 Å; Yang *et al.*, 1997).

The X-ray data of RMP-pepstatin A complex were collected to a maximum resolution of 2.7 Å at beamline X12C, Brookhaven National Laboratory, New York, USA. The wavelength used for data collection was 1.15 Å. The data were processed using *DENZO* and *SCALEPACK* (Otwinowski, 1993). A total of 43156 reflections with non-zero intensities to 2.7 Å were merged to yield 9360 unique reflections. The $R_{\rm merge}$ is 0.092 for symmetry-equivalent reflections based on intensities and the completeness of the data set is 84.9 up to 2.7 Å resolution. For the highest resolution shell (2.80–2.70 Å), the value of $R_{\rm merge}$ is 0.159 and the completeness of data is 47.9%.

### 2.2. Structure determination and refinement

The coordinates of the native RMP enzyme (Yang *et al.*, 1997) were used as the starting model. In the refinement, 8599 reflections in the resolution range 8–2.7 Å were used. In the first cycle of refinement rigid-body refinement was applied to the model, after which the $R$ value was 28.2%. The model was then refined using the *X-PLOR* package (Brünger, 1992*a*) using the slow-cooling protocol. The $R$ value dropped to 25.0% after this refinement. A *SIGMAA*-weighted $\Delta F$ map (Read, 1986) was calculated. The map was examined using the *TURBO-FRODO* program (Roussel *et al.*, 1990) and the positions of the pepstatin A molecule and the carbohydrate moieties bound to residues Asn79 and Asn188 were located from the $\Delta F$

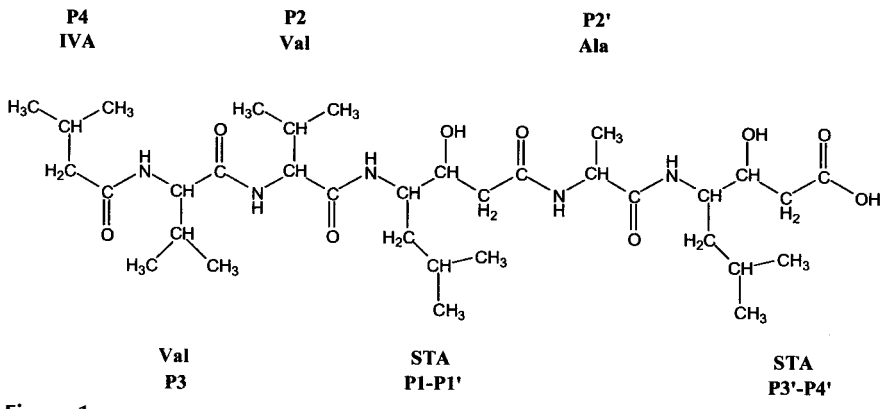


**Figure 1**
The chemical structure of pepstatin A (Umezawa *et al.*, 1970).

**Table 1**
*X-PLOR* refinement results.

| | |
|---|---|
| Number of protein non-H atoms | 2665 |
| Number of carbohydrate non-H atoms | 39 |
| Number of inhibitor non-H atoms | 48 |
| Resolution range (Å) | 2.7–8.0 |
| Number of unique reflections used in refinement | 8599 |
| *R* value (all data) (%) | 19.3 |
| $R_{free}$ (5% of all data) (%) | 28.0 |
| R.m.s.d. for bond distances (Å) | 0.01 |
| R.m.s.d. for bond angles (°) | 1.7 |
| R.m.s.d. for dihedral angles (°) | 27 |
| R.m.s.d. for impropers (°) | 1.8 |
| Average *B* factor for the enzyme (Å$^2$) | 32.3 |
| Average *B* factor for N-terminal domain (Å$^2$) | 25.1 |
| Average *B* factor for C-terminal domain (Å$^2$) | 39.8 |
| Average *B* factor for carbohydrate (Å$^2$) | 70.7 |
| Average *B* factor for the inhibitor (Å$^2$) | 76.1 |
| Average *B* factor for the active-site surface flap (Å$^2$) | 51.7 |
| Average *B* factor for the flexible sub-domain (Å$^2$) | 45.3 |
| Average *B* factor for the residues in the C-terminal domain except those of the flexible sub-domain (Å$^2$) | 28.6 |

map. The complex model was then subjected to six cycles of simulated-annealing refinement and 16 cycles of positional refinement with all the non-zero intensity reflections in the resolution range 8–2.7 Å. The refinements were interspersed with manual model building and adjustments. The free *R* factor (Brünger, 1992*b*) was calculated from the second to the second-last cycles of refinements by omitting randomly about 5% of the observed data (432 reflections). The $R_{free}$ dropped from 34.2% on the second cycle of refinement to 28.0% on the second-last cycle of refinement. In the final cycle of refinement, all reflections were used and *R* was 19.3%. No solvent molecules were added to the model during the refinement. Eight bins of data were used. The highest resolution-range bin was 2.70–2.82 Å and contained 515 reflections in the working set and 24 reflections in the test set for $R_{free}$. In this bin, *R* refined to 29.8% and $R_{free}$ refined to 31.4%. The final results of the refinement are listed in Table 1. The coordinates and structure factors have been deposited with the Protein Data Bank.

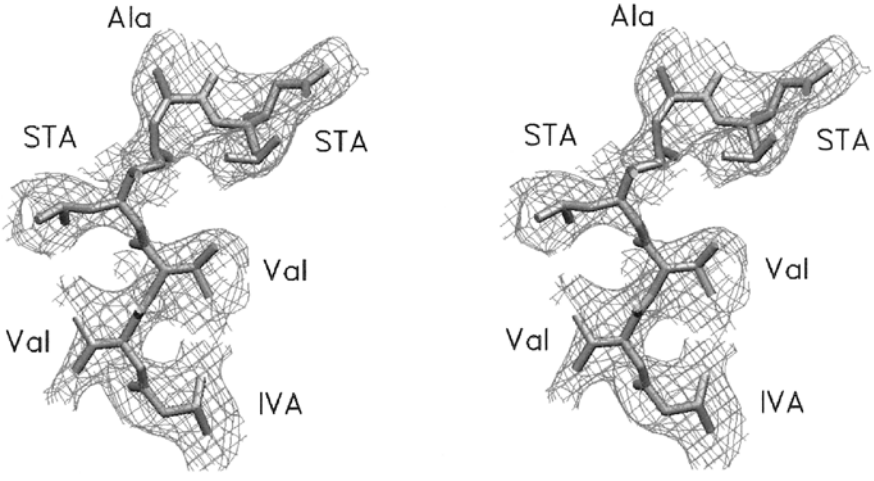


**Figure 2**
Electron-density map ($2F_o - F_c$) at the pepstatin A site. This figure was prepared using *SETOR* (Evans, 1993).

## 3. Results and discussion

### 3.1. Quality of the final model

The structure of RMP complexed with pepstatin A has been refined to a crystallographic *R* value of 19.3% and an $R_{free}$ of 28.0% at 2.7 Å resolution. Three N-terminal residues and the side chains of 12 residues are omitted in the refinement owing to insufficient indication of their positions in the final electron-density map. An electron-density map ($2F_o - F_c$) at the inhibitor pepstatin A site is shown in Fig. 2. The final model was also examined for the main-chain torsion angles ($\varphi$, $\psi$) by the program *PROCHECK* (Laskowski *et al.*, 1993). A Ramachandran plot (Ramachandran & Sasisekharan, 1968) produced by the program *PROCHECK* is shown in Fig. 3. All amino-acid residues are in the allowed regions.

### 3.2. Comparison with the native enzyme

RMP contains two domains of approximately the same number of residues (N-terminal domain 1–186; C-terminal domain 187–361). The active site and the substrate-binding site are located in a deep cleft situated between the two domains. RMP has a flexible sub-domain (residues 211–331) within the C-terminal domain. The presence of a flexible sub-domain has also been observed in other aspartic proteinases (Šali *et al.*, 1989; Sielecki *et al.*, 1990; Cooper *et al.*, 1990; Abad-Zapatero *et al.*, 1991). We superimposed the coordinates of the complex structure with the coordinates of the native enzyme. The two domains of RMP did not show any movement in the complex structure with respect to the native enzyme. No movement of the sub-domain was observed either. As we observed only the initial and final stages of the inhibitor binding, we do not know whether there are any domain movements during the binding process. The average *B* factor for the flexible sub-domain is 45.3 Å$^2$, which is 9.5 Å$^2$ lower than average *B* factor of the sub-domain in the native enzyme. This indicates that the sub-domain becomes less flexible on binding pepstatin A. The active-site flap (residues 82–88) underwent a dramatic conformational change, moving towards the inhibitor and forming two hydrogen bonds with it. The flap covers positions P2–P1′. Its residues are involved in the formation of subsites S2, S1 and S2′. Residue 85 could not be modelled in native RMP, but the entire flap with no breaks could be modelled in the complex. The average *B* factor of the flap (51.7 Å$^2$) in the complex structure is much lower than in the native structure (66.6 Å$^2$), which suggests the flap becomes more rigid in the complex.

### 3.3. Hydrogen bonds

The inhibitor pepstatin A makes ten hydrogen bonds with the enzyme; a schematic diagram of these hydrogen bonds is shown in Fig. 4. The hydroxyl group at the

C3 position of statine P1–P1′ replaces the conserved water molecule at the enzyme active site and forms hydrogen bonds with both of the catalytic aspartate residues (Asp38 and Asp237). C3 of the statine residue is in the *S*-configuration. This type of conformation has also been observed in other aspartic proteinase–statine-type inhibitor complexes (Cooper *et al.*, 1989; Šali *et al.*, 1989; Bailey *et al.*, 1993) and mimics the expected transition state of the enzyme–substrate action. The active-site flap moves towards the pepstatin A molecule and forms two strong hydrogen bonds with the inhibitor: the N—H of Gly83 with the P1′ CO group and N—H of Thr84 with the P2 CO group. The formation of these two hydrogen bonds increases the rigidity of this flexible surface flap. The side chain of Thr240 rotates about 90° along the C$\alpha$—C$\beta$ bond axis to form two hydrogen bonds with the P1 NH and P3 CO groups, respectively. Asn241 forms a hydrogen bond with the P3 NH group using its O$^{\delta}$ atom and Gly40 forms a hydrogen bond with the P2′ NH group.

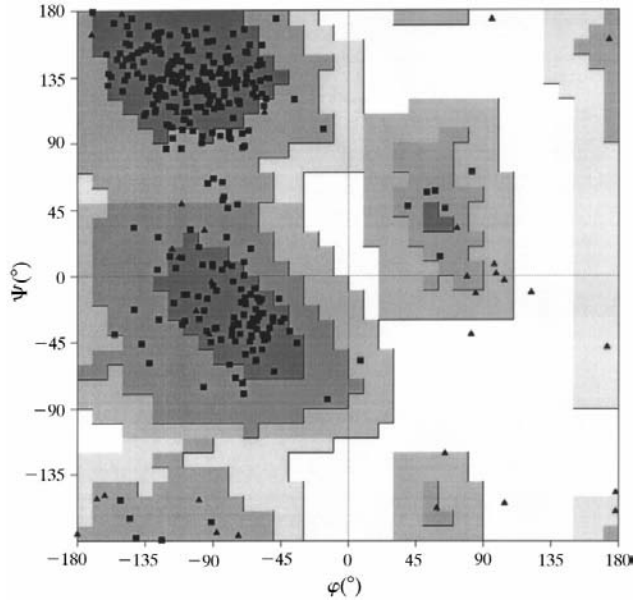


**Figure 3**
Ramachandran plot (Ramachandran & Sasisekharan, 1968) of the complex generated by *PROCHECK* (Laskowski *et al.*, 1993). The glycines are shown as triangles.

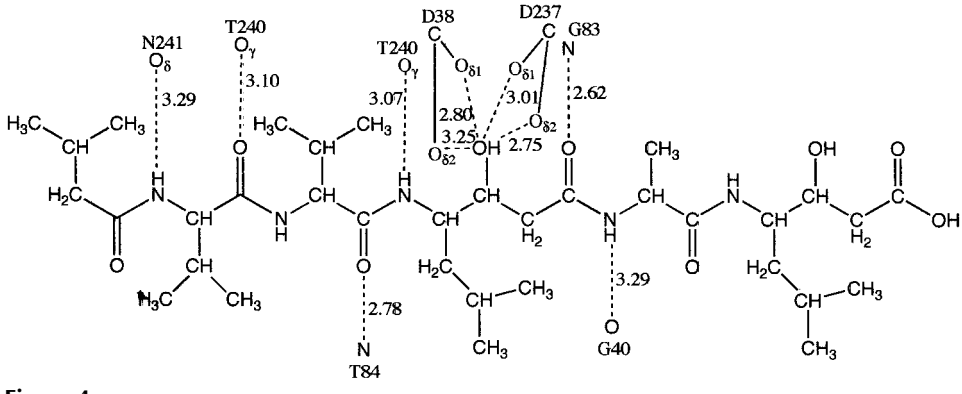


**Figure 4**
Schematic representation of the hydrogen bonds formed between pepstatin A and RMP in the complex structure.

**Table 2**
van der Waals contacts between the RMP and pepstatin A ($d \leq 4.11$ Å).

Calculated using the program *CONTACSYM* (Sheriff *et al.*, 1989; Sheriff, 1993) with maximum limit for van der Waals contacts of 4.11 Å.

| Pepstatin A | Position | Residues of RMP which make van der Waals contacts with pepstatin A |
|---|---|---|
| IVA | P4 | Leu321 |
| Val | P3 | Glu19, Pro117, Gly239, Thr240, Asn241 |
| Val | P2 | Gly83, Thr84, Thr240, Gly325, Ile329 |
| STA | P1–P1′ | Leu36, Asp38, Gly40, Tyr82, Gly83, Pro117, Leu132, Asp237, Gly239 |
| Ala | P2′ | Gly40, Tyr82, Asn140, Phe210 |
| STA | P3′–P4′ | Phe210, Thr235, Asp237, Ile329 |

### 3.4. The $\gamma$-turn in pepstatin A

When the CO group of a residue *i* forms a hydrogen bond with the NH group of another residue $i + 2$, a $\gamma$-turn is formed. There are two types of $\gamma$-turns, classic and inverse (Milner-White *et al.*, 1988). The CO group of the statine residue at P1–P1′ forms a hydrogen bond with the NH group of the statine residue at P3′–P4′ and, therefore, an inverse $\gamma$-turn is formed in pepstatin A. The reason for the formation of this inverse $\gamma$-turn in pepstatin A is that the leucyl side of the P3′–P4′ statine residue binds back into the S1′ subsite. The formation of a $\gamma$-turn in the pepstatin A molecule is also observed in other aspartic proteinase–pepstatin A complexes (Suguna *et al.*, 1992; Bailey *et al.*, 1993).

### 3.5. Binding subsites

Pepstatin A fits into the substrate-binding cleft between the two domains of RMP in an extended conformation upon binding to the enzyme. Both C3 atoms of the statine residues are in the *S*-configuration. Previous studies (Rich *et al.*, 1980; Boger *et al.*, 1983; Bailey *et al.*, 1993) suggest that the 3*S* enantiomers of the statine residue at the P1–P1′ position are much more potent than the 3*R* enantiomers for pepstatin-type inhibitors. Our present study is consistent with these studies and suggests that RMP is also stereoselective in binding with pepstatin-type inhibitors. A stereo superposition of the inhibitor complex and the native structure is shown in Fig. 5, and a stereo representation of the hydrogen bonding of RMP to the pepstatin A molecule is shown in Fig. 6. The subsites' residues which make van der Waals contacts with the inhibitor ($d \leq 4.11$ Å) are listed in Table 2. A stereo representation of the van der Waals contacts of RMP with the pepstatin A molecule is shown in Fig. 7. Since pepstatin A contains two dipeptide-analogue statine residues at the P1–P1′ and

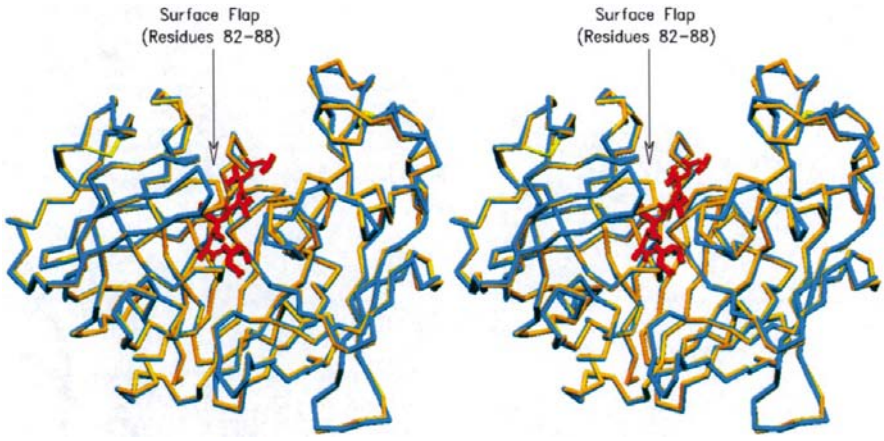


**Figure 5**
Stereo superposition of the complex structure with the native enzyme structure. The native enzyme, the complexed enzyme and the inhibitor pepstatin A are shown in blue, orange and red, respectively. This figure was prepared using *SETOR* (Evans, 1993).

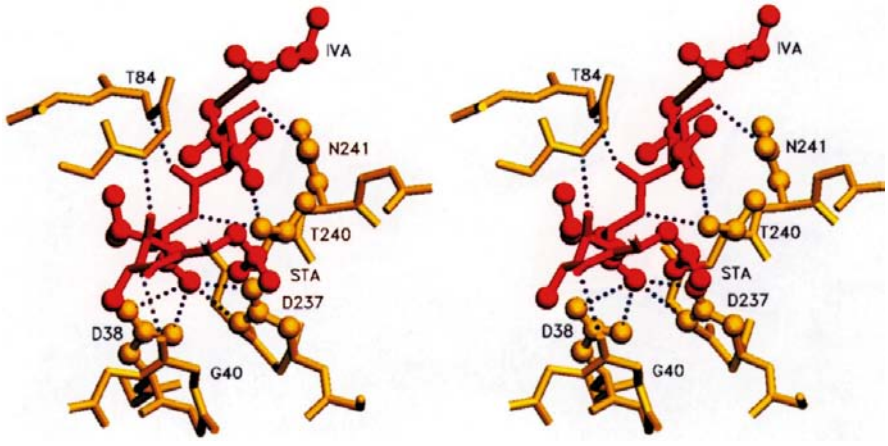


**Figure 6**
Stereo representation (same orientation at Fig. 5) of the inhibitor pepstatin A (red) of the RMP complex with associated hydrogen bonded RMP residues (orange). This figure was prepared using *SETOR* (Evans, 1993).

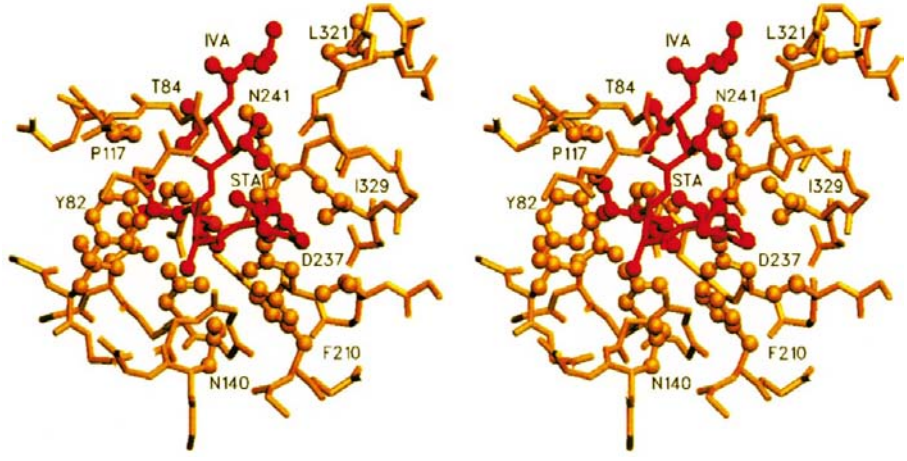


**Figure 7**
Stereo representation (same orientation at Fig. 5) of the inhibitor pepstatin A (red) of the RMP complex with RMP residues (orange) within 4.11 Å. This figure was prepared using *SETOR* (Evans, 1993). Insufficient electron density was available to model the sidechain of T84.

P3′–P4′ positions, it should interact with the S4 to S4′ subsites of the enzyme. However, in the RMP–pepstatin A complex the statine residue at P1–P1′ does not have a side chain to occupy the binding subsite S1′, and the leucine-like side chain of the statine residue at P3′–P4′, which should interact with subsite S3′, binds back into subsite S1′ and forms an inverse $\gamma$-turn in the inhibitor. Owing to the movement of the leucyl side chain, the carboxyl group of this statine residue is also oriented away from the subsite S4′ and is pointing towards the solvent. In the complex, the active-site flap (residues 82–88) undergoes a significant conformational change, moving close to the inhibitor and covering positions P2–P1′. Its residues are involved in the formation of subsites S2, S1 and S2′. This flap becomes rigid owing to the formation of hydrogen bonds and van der Waals interactions with the inhibitor. Residue Tyr82 is involved in the formation of subsites S2′ and S1 and separates these two subsites. At the S4 subsite, Leu321 moves about 0.5–0.7 Å toward the side chain of IVA to make good van der Waals contacts. Residue Ile244 is about 5 Å from IVA and forms part of the subsite. This suggests that modifications to a large group at the P4 position of the inhibitor may result in better contacts with the subsite and confer stronger inhibition. The IVA side chain also interacts with P2 valine residue by van der Waals contacts ($d$ = 3.8 Å). At subsite S3, the subsite residues make good interactions with the side chain of the valine residue at the P3 position of the inhibitor. Residue Leu17, which may be involved in the formation of the S3 subsite, is about 4–5 Å from the side chain of the valine residue and therefore leaves room for further modification. The inhibitor is tightly bound in the central region and loosely bound at both ends.

This research is supported by a research grant from the Natural Sciences and Engineering Research Council of Canada (to JWQ). JY acknowledges the University of Saskatchewan for the awarding of a

postgraduate scholarship. The authors would also like to thank Dr Palle Schneider, Novo Nordisk, Denmark, for providing the purified RMP enzyme and Dr Robert M. Sweet, Brookhaven National Laboratory, New York, USA, for his help with the data collection.

## References


Abad-Zapatero, C., Rydel, T. J., Neidhart, D. J., Luly, J. & Erickson, J. W. (1991). *Adv. Exp. Med. Biol.*, **306**, 9–21.

Bailey, D., Cooper, J. B., Veerapandian, B., Blundell, T. L., Atrash, B., Jones, D. M. & Szelke, M. (1993). *Biochem. J.* **289**, 363–371.

Baudys, M., Foundling, S., Pavlik, M., Blundell, T. & Kostka, V. (1988). *FEBS Lett.* **235**, 271–274.

Boger, J., Lohr, N. S., Ulm, E. H., Poe, M., Blaine, E. H., Fanelli, G. M., Lin, T.-Y., Payne, L. S., Schorn, T. W., LaMont, B. I., Vassil, T. C., Stabilito, I. I., Veber, D. F., Rich, D. H. & Bopari, A. S. (1983). *Nature (London)*, **303**, 81–84.

Brünger, A. T. (1992*a*). *X-PLOR Manual Version 3.1*. Yale University, USA.

Brünger, A. T. (1992*b*). *Nature (London)*, **55**, 472–475.

Cooper, J. B., Foundling, S. I., Blundell, T. L., Boger, J., Jupp, R. A. & Kay, J. (1989). *Biochemistry*, **28**, 8596–8603.

Cooper, J. B., Kahn, G., Taylor, G., Tickle, I. J. & Blundell, T. L. (1990). *J. Mol. Biol.* **214**, 199–222.

Evans, S. V. (1993). *J. Mol. Graph.* **11**, 134–138.

Foundling, S. I., Cooper, J., Watson, F. E., Cleasby, A., Pearl, L. H., Sibanda, B. L., Hemmings, A., Wood, S. P., Blundell, T. L., Valler, M. J., Norey, C. G., Kay, J., Boger, J., Dunn, B. M., Leckie, B. J., Jones, D. M., Atrash, B., Hallett, A. & Szelke, M. (1987). *Nature (London)*, **327**, 349–352.

Foundling, S. I., Cooper, J., Watson, F. E., Pearl, L. H., Hemmings, A., Wood, S. P., Blundell, T., Hallett, A., Jones, D. M., Suerias, J., Atrash, B. & Szelke, M. (1987). *J. Cardiovasc. Pharmacol.* **10** Suppl. 7, S59–S68.

Hoover, D. J., Veerapandian, B., Cooper, J. B., Damon, D. B., Dominy, B. W., Rosati, R. L. & Blundell, T. L. (1991). *Adv. Exp. Med. Biol.* **306**, 269–273.

James, M. N. G. & Sielecki, A. R. (1985). *Biochemistry*, **24**, 3701–3713.

Jia, Z., Vandonselaar, M., Schneider, P. & Quail, J. W. (1995). *Acta Cryst.* D**51**, 243–244.

Laskowski, P. A., MacArthur, M. W., Hutchinson, S. G. & Thornton, J. M. (1993). *J. Appl. Cryst.* **26**, 283–291.

Milner-White, E., Ross, B. M., Ismail, R., Belhadj-Mostefa, K. & Poet, P. (1988). *J. Mol. Biol.* **204**, 777–782.

Newman, M., Watson, F., Roychowdhury, P., Jones, H., Badasso, M., Cleasby, A., Wood, S. P., Tickle, I. J. & Blundell, T. L. (1993). *J. Mol. Biol.* **230**, 260–283.

Otwinowski, Z. (1993). *Data Collection and Processing. Proceedings of the CCP4 Study Weekend*, edited by L. Sawyer, N. Isaacs & S. Bailey, pp. 56–62. Warrington: Daresbury Laboratory.

Pitts, J. E., Crawford, M. D., Nugent, P. G., Wester, R. T., Cooper, J. B., Mantyla, A., Fagerstrom, R. & Nevalainen, H. (1995). *Adv. Exp. Med. Biol.* **362**, 543–547.

Quail, J. W., Yang, J., Schneider, P. & Jia, Z. (1998). *Adv. Exp. Med. Biol.* **436**, 283–292.

Ramachandran, G. N. & Sasisekharan, V. (1968). *Adv. Protein Chem.* **23**, 283–437.

Read, R. J. (1986). *Acta Cryst.* A**42**, 140–149.

Rich, D. H., Sun, E. T. O. & Ulm, E. (1980). *J. Med. Chem.* **23**, 27–33.

Roussel, A., Fontecilla-Camps, J. C. & Cambillau, C. (1990). *Acta Cryst.* A**46**, C66.

Šali, A., Veerapandian, B., Cooper, J. B., Foundling, S. I., Hoover, D. J. & Blundell, T. L. (1989). *EMBO J.* **8**, 2179–2188.

Sheriff, S. (1993). *Immunomethods*, **3**, 191–196.

Sheriff, S., Hendrickson, W. A. & Smith, J. L. (1989). *J. Mol. Biol.* **197**, 273–296.

Sielecki, A. R., Fedorov, A. A., Boodhoo, A., Andreeva, N. S. & James, M. N. G. (1990). *J. Mol. Biol.* **214**, 143–170.

Suguna, K., Padlan, E. A., Bott, R., Boger, J., Parris, K. D. & Davies, D. R. (1992). *Proteins*, **13**, 195–205.

Suguna, K., Padlan, E. A., Smith, C. W., Carlson, W. D. & Davies, D. R. (1987). *Proc. Natl Acad. Sci. USA*, **84**, 7009–7013.

Thaller, C., Weaver, L. H., Eichele, G., Wilson, E., Karlsson, R. & Jansonius, J. N. (1981). *J. Mol. Biol.* **147**, 465–469.

Umezawa, H., Aoyagi, T., Morishima, M., Matsuzaki, M. & Hamada, M. (1970). *J. Antibiot. Tokyo*, **23**, 259–262.

Veerapandian, B., Cooper, J. B., Šali, A., Blundell, T. L., Rosati, R. L., Dominy, B. W., Damon, D. B. & Hoover, D. J. (1992). *Protein Sci.* **1**, 322–328.

Yang, J., Teplyakov, A. & Quail, J. W. (1997). *J. Mol. Biol.* **268**, 449–459.